Liquid Crystals
Publication details, including instructions for authors and subscription information:
http://www.informaworld.com/smpp/title~content=t713926090

Induced smectic A_1, A_2 and Ã phases at low temperatures. Molecule parameters related to phase diagrams and structure

J. M. Auguste[a]; G. Sigaud[a]
[a] Centre de Recherche Paul Pascal, Université de Bordeaux I, Talence Cedex, France

To cite this Article Auguste, J. M. and Sigaud, G.(1989) 'Induced smectic A_1, A_2 and Ã phases at low temperatures. Molecule parameters related to phase diagrams and structure', Liquid Crystals, 6: 2, 185 — 197
To link to this Article: DOI: 10.1080/02678298908033213
URL: http://dx.doi.org/10.1080/02678298908033213

Liquid Crystals, 1989, Vol. 6, No. 2, 185–197

Induced smectic A_1, A_2 and $\tilde{A}$ phases at low temperatures

Molecule parameters related to phase diagrams and structure

by J. M. AUGUSTE and G. SIGAUD
Centre de Recherche Paul Pascal, Université de Bordeaux I,
F-33405 Talence Cedex, France

(*Received 16 January 1989; accepted 21 March 1989*)

Binary mixtures combining some rod-like mesogens with non-mesogenic plate-like molecules show surprising induction of smectic A phases close to room temperature. We have systematically varied the nature of both components in order to correlate the phenomenon to the molecular structure. The calorimetric and X-ray analysis of several systems specify the topologies of the phase diagrams and definitely confirm the unusual character of these phases.

1. Introduction

The observation of the evolution of liquid-crystalline properties through the investigation of binary phase diagrams has shown at an early stage that the smectic A phase can be strongly stabilized in mixtures [1], the maximum transition temperature increasing by several tens of degrees compared to the corresponding temperature in the pure compound(s); thus enhancing the smectic phase [2]. In a few cases it may happen that none of the components is smectic, yet the mixtures are in some range of concentration; the phase is induced [3]. Most of these phenomena have been obtained in mixtures of two rod-like crystals, one polar and the second non-polar, and far fewer with two non-polar mesogens [4]. A theoretical interpretation has been proposed which considers a more or less weak complex formation between the two kinds of molecules [5, 6] which implies an important influence of the chemical structure. However, it appears from our recent studies that enhanced smectic A phases are now common in systems combining a comb-like liquid-crystalline polymer and a low molecular weight rod-like liquid crystal even though the latter is chemically related to the mesogenic parts of the macromolecule [7, 8]. Moreover the increase in the transition temperature is clearly related to large variations of the layer spacing. Thus, the structural characteristics of both components are also of some importance in order to provide favourable interactions to stabilize the layered arrangement.

The binary mixtures with an induced smectic A phase which we have described in two previous papers [9, 10] depart from these classical combinations, they occur in binary systems between a polar, rod-like mesogen and a plate-like non-mesogenic compound, and result in phases of various types, namely S_{A_1}, S_{A_2}, $S_{\tilde{A}}$ [11]. In the present work we investigate systematically these kinds of phase diagrams by varying the molecular structure of the components in order to specify first the conditions in which this non-ideal behaviour is reproducible. Thus, to learn about the trends for these different systems in inducing a phase we use the contact method and we correlate the rough topologies of the phase diagrams to the changes in the nature of the components. Once the induced phases have been detected, they are then characterized through the study of mixtures with definite compositions by optical microscopy, differential scanning calorimetry and X-ray diffraction. In the last part of the experimental section the phase diagrams of two model systems are fully described providing quantitative data on the location of the induced domains and the variation of the layer spacings with mole fraction. All of these results are discussed in order to understand what the structure of a S_A phase combining such different compounds could be.

2. Influence of the nature of the components upon phase induction

2.1. *Selection of the constituents*

This choice is driven by our preliminary studies of mixtures of rod-like and plate-like molecules [9, 12]. These investigations have shown, in particular, a phase induction with fully saturated liquid crystals from the cyanobicyclohexyl family, and surprisingly not with the cyanobiphenyl homologues containing an aromatic core. The second component is a substituted polycyclic compound of moderate size namely three to four condensed rings. The role of the aliphatic chain and the polar or non-polar character of the mesogen upon phase induction can be tested since a large variety of bicyclohexyl derivatives are commercially available. On the other hand it is possible to procure polycyclic molecules with various configurations (location of the rings) and substituents (nature, number, place).

Table 1. Mesogenic compounds.

Name	Formula	Merck Index	Polymorphism
Trans-4′-ethyl-bicyclohexyl-4-carbonitrile		CCH2	$N \xrightarrow{44{\cdot}1°C} I$
Trans-4′-propyl-bicyclohexyl-4-carbonitrile		CCH3	$N \xrightarrow{81°C} I$
Trans-4′-butyl-bicyclohexyl-4-carbonitrile		CCH4	$S_B \xrightarrow{(54°C)} N \xrightarrow{78{\cdot}8°C} I$
Trans-4′-pentyl-bicyclohexyl-4-carbonitrile	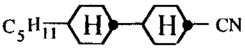	CCH5	$S_B \xrightarrow{(51{\cdot}3°C)} N \xrightarrow{86{\cdot}3°C} I$
Trans-4′-heptyl-bicyclohexyl-4-carbonitrile		CCH7	$S_B \xrightarrow{(41°C)} N \xrightarrow{81{\cdot}7°C} I$
Trans-4′-butyl-bicyclohexyl-4-heptyl-4′-carbonitrile	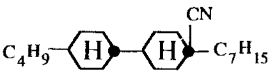	CCN47	$S_{A1} \xrightarrow{(30{\cdot}7°C)} N \xrightarrow{58{\cdot}8°C} I$
Trans-4′-pentyl-bicyclohexyl-4-pentyl-4′-carbonitrile	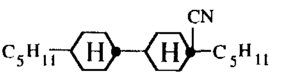	CCN55	$N \xrightarrow{64{\cdot}1°C} I$
Trans-4′-pentyl-bicyclohexyl-4-pentyl-4′-carboxylate	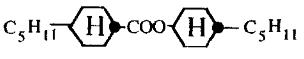	OS55	$S_B \xrightarrow{69{\cdot}8°C} I$

Table 2. Polycyclic non-mesogenic compounds.

Name	Formula	Abbreviation	Melting point/°C
1-Aminopyrene	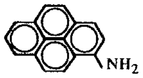	1AP	112
3-Amino fluoranthene	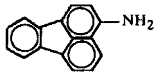	3AF	117
1-Amino-9 fluorenone	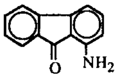	1A9F	119
2-Amino-9 fluorenone	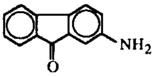	2A9F	158
2-Amino fluorene	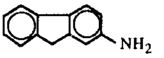	—	126
2,7-Diamino fluorene	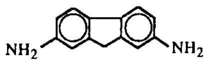	2,7DAF	161
2-Aminopyrene	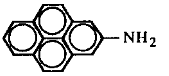	2AP	120
9-Amino phenantrene	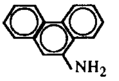	9APh	138
1-Pyrene carboxaldehyde	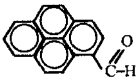	—	124
4-Pyrene ethanol	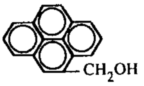	CH_2OHP	123
1-Hydroxy-9 fluorenone	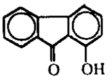	—	119
2-Hydroxy-9 fluorenone	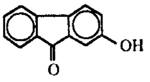	—	205

The choice of mesogenic compounds is reported in table 1. The name, chemical formula and an abbreviation are given for each compound which we have used. Table 2 offers the same information for the polycyclic compounds. (All products are commercially available from MERCK for the bicyclohexyls and from ALDRICH for the polycyclic ones. The purity ranges between 97 and 99 per cent for the latter; they have been used without further purification.) In the former table the sequence of liquid-crystalline phases for the pure material is also indicated.

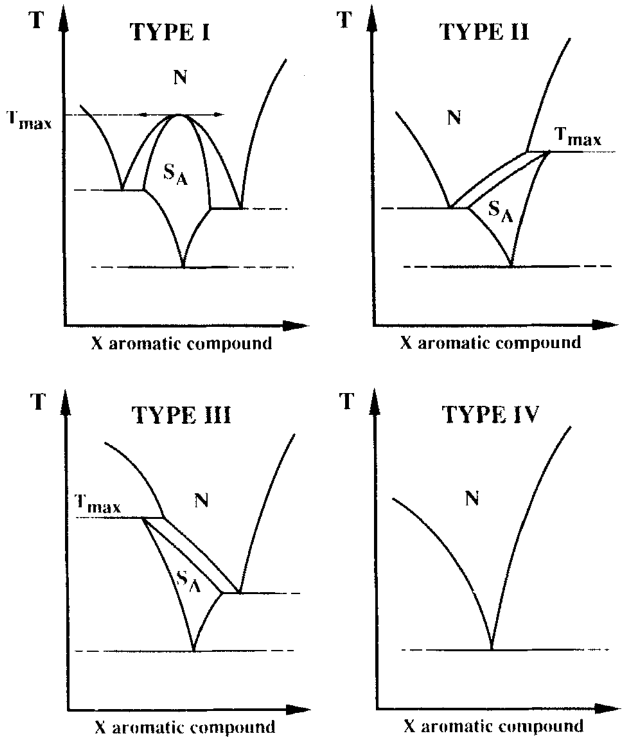

Figure 1. Topologies of the four types of phase diagram.

2.2. *Topology of the binary phase diagrams*

Generally speaking, the phase diagrams have been constructed by the use of the contact method and can be classified into four different types which are described in figure 1. The phase diagram as constructed by the contact method are consequently simplified. We know that in many cases they are likely to present several joined S_A domains (S_{A_1}, S_{A_2}, $S_{\tilde{A}}$). These are impossible to detect through microscopic observation of a contact sample since their textures are undifferentiated under these conditions. But this deficiency of the contact method has no importance at this stage since the study of the topology is detailed further by the analysis of definite compositions once we had decided that it deserves further attention. The four types of behaviour are (figure 1)

type I: induced S_A phase with a maximum;
type II: induced S_A phase without an observable maximum;
type III: S_A phase at low temperatures without enhancement;
type IV: no S_A phase, simple nematic eutectic.

The main features of about thirty diagrams are summarized in the table 3 in order to correlate their characteristics to the nature of the two components. All diagrams have been established upon cooling, several smectic A phases being monotropic with respect to the stable crystalline form of the mesogenic compound.

2.3. *Comments*

Table 3 shows the zone of phase diagrams with induced phases, that is type I, which is of interest. This part corresponds to binary combinations between mesogenic

Table 3. Correlations between the type of phase diagram observed (I, II, III, IV: cf. figure 1) and the components of the binary system. When given, the temperature corresponds to the maximum stability of the smectic A phase (I, II, III only).

	CCH2	CCH3	CCH4	CCH5	CCH7	CCN47	CCN55	OS55
1-Aminopyrene		IV	I 67·5°C	I 55°C	I 51°C			
3-Amino fluoranthene	IV	I 54°C	I 68·5°C	I 58°C	I 54°C	IV	IV	IV
1-Amino-9 fluorenone	IV	IV	I 60°C	I 54·5°C	IV	IV	IV	
2-Amino-9 fluorenone			III 50°C	II 49·5°C				
2-Amino fluorene			IV		II 62°C			
2,7-Diamino fluorene			II 61·5°C		II 43°C		IV	
2-Aminopyrene			II 50°C					
9-Amino phenantrene			III 39°C					
1-Pyrene carboxaldehyde			III 43°C					
4-Pyrene ethanol			III 45°C					
1-Hydroxy-9 fluorenone			III 39°C		IV		IV	IV
2-Hydroxy-9 fluorenone			IV					

molecules and polycyclic compounds with well-defined chemical structures. Regarding the characteristics of the liquid crystal, we consider the following as relevant for phase induction.

The polarity of the molecule. A polar cyano head group located along the axis of the molecule seems necessary; neither of the compounds CCN47 and CCN55 with a polar function off axis, nor the compound OS55 which is non-polar, induce a smectic phase.

The length of the aliphatic tail. Figure 2 shows the evolution of the temperature at the maximum of the S_A–N phase line as a function of size of the chain in the CCH compound for different associations with aromatic molecules. It turns out that a C_4 sequence is more stabilizing.

The important parameters are more difficult to demonstrate in polycyclic compounds. However the NH_2 substituent appears the most relevant and its location on the aromatic structure plays an obvious role: 1A9F induces a S_A phase whereas 2A9F does not. Moreover two amino substituents on the same molecule do not improve the stabilization of the S_A phase (see CCH4-2,7 diaminofluorene). We note that aromatic compounds smaller or larger than the mean size of the selected members in table 2 failed to induce a smectic phase.

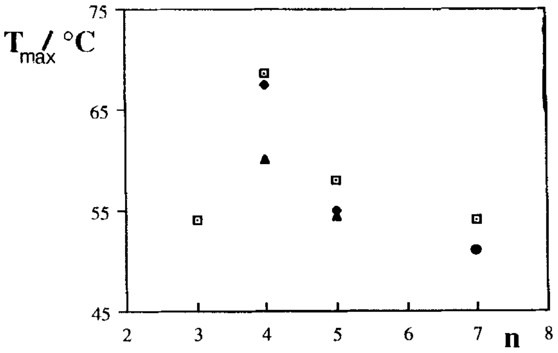

Figure 2. Evolution of the temperature at the maximum of the induced phase as a function of the aliphatic chain length (n) of the mesogen CCHn. □ represents 3AF, ◆ 1AP and ▲ 1A9F.

Thus, the qualitative conclusion of this first part is that both compounds must fulfil conditions in polarity (terminal CN/NH_2 substituent) and size (chain length/number of condensed rings).

3. Characterization of mixtures at a definite concentration

Because of the previous results we have easily selected several interesting combinations which offer an induced S_A. Some preliminary trials with these systems have shown that the monophasic domain of the induced phase ranges between 0·1 and 0·2 expressed in the molar fraction of the plate-like compound (this generalizes the very unusual solubility of such aromatic compounds in aliphatic cyanobicyclohexyls previously pointed out). (Beyond some concentration we can directly verify by optical means that the aromatic compound is no longer miscible: some microcrystalline parts remain clearly visible in the isotropic state. Of course we always limited our studies to much lower mole fractions.) The mixtures chosen were analysed by the three classified techniques in use to characterize a liquid crystal: polarized optical microscopy, small angle X-ray diffraction and differential scanning calorimetry. Each of the following paragraphs provides a general comment of the peculiarities of the observations obtained with each type of technique. The results are summed in table 4 at the end of this section.

3.1. *Polarized optical microscopy*

The textural changes between nematic and induced smectic A phases present some unusual features; starting from a homeotropic sample in the nematic phase, we observed at the transition the growth of bâtonnets leading to a fan-shaped texture and complete loss of homeotropy. It is quite unexpected that the direction of the optical axis changes in that way at the S_A–N transition (the common case is the reverse). Indeed, this behaviour is generally associated with phase changes between a nematic and an ordered mesophase (S_B–N for example). It is also worth noting that the mixtures often exhibit biphasic domains extending over several degrees which indicate the first order character for the S_A–N transition, rarely observed in this case.

3.2. *Differential scanning calorimetry*

The enthalpies at the N–I and induced S_A–N transitions are reported in table 4 for the different systems. For the N–I transition, the values are comparable to those

Table 4. Characteristics of the different binary systems: transition temperatures ([ ]: monotropic transitions); enthalpies of transitions; nature of S_A phases; layer spacings.

	Microscopy		D.S.C.		X-Rays	
Mixtures	$T_{S_A\text{-}N}$/°C	$T_{N\text{-}I}$/°C	$\Delta H_{S_A\text{-}N}$/ kJ mol^{-1}	$\Delta H_{N\text{-}I}$/ kJ mol^{-1}	Layer spacing/Å	Type of S_A
CCH3-3AF	[54·2]	75·2	2·37	0·44	13·1	S_{A_2}
x = 0·183					26·3	
CCH4-3AF	62·5	78·4	3·05	0·66	13·8	S_{A_2}
x = 0·167					27·7	
CCH4-1AP	60·1	78·2	2·9	0·52	13·6	S_{A_2}
x = 0·164					27·3	
CCH4-2AP	[53·6]	77·8		0·81	13·8	S_{A_2}
x = 0·146					27·8	
CCH4-1A9F	[56·6]	80·3	2·08	0·57	13·9	S_{A_1}
x = 0·124						
CCH4-CH2OHP	[40]	69·5	0·68	0·51		
x = 0·18						
CCH4-9APh	[28·9]	65·5		0·36		
x = 0·18						
CCH4-2,7DAF	[63·1]	82·7	2·11	0·57	14·4	S_{A_1}
x = 0·18						
CCH5-2A9F	[49·2]	83·8	1·23	0·47	15·6	S_{A_1}
x = 0·178						
CCH7-3AF	[53·9]	82·7	0·72	0·58	16·4	S_{A_2}
x = 0·18					32·8	

commonly measured in pure liquid crystals (for example $\Delta H_{N\text{-}I} = 1{\cdot}02\,\mathrm{kJ\,mol^{-1}}$ for the compound 5O8). In contrast the scale in figure 3 shows that the molar enthalpies for the S_A–N transitions (A_1 and A_2 as well) are exceptionally high (more than twice the value for a S_{A_2}–N in usual polar systems although the molecular weight is much lower). Moreover, large differences appear from one system to the other (the transitional enthalpy of the mixture CCH4-3AF is four times that for CCH7-3AF; see table 4). This large heat excess at the S_A–N transition together with the noticeable width of the S_A–N spindles (5–10°C) corroborates the assumption of a strong first order character. The vicinity of the nematic–isotropic transition cannot explain this exceptional enthalpy: the nematic range is at least 15°C at the highest point of the N–S_A equilibrium curve. It is also remarkable that this heat is higher than that obtained with S_A–I transition (see figure 3).

Finally, the calorimetric study has also given evidence for a S_{A_1}–$S_{\tilde{A}}$ transition in the system CCH4-1A9F: the thermogram in figure 4 indicates that a weak energy is associated with this phase change but no biphasic domain corresponds to this peak. Nevertheless a high resolution study performed by THOEN *et al.* [10] has classified the transition as weakly first order.

3.3. *X-ray characterization: analysis of the layer spacings*

The analysis of diffraction patterns indicates that the induced S_A phases are either of S_{A_1} type with a single order of reflection (CCH4-1A9F), or of S_{A_2} type with two commensurate orders of reflection (CCH4-1AP). The signature of the S_{A_1}–$S_{\tilde{A}}$ transition in the mixture CCH4-1A9F is an additional Bragg spot incommensurate with

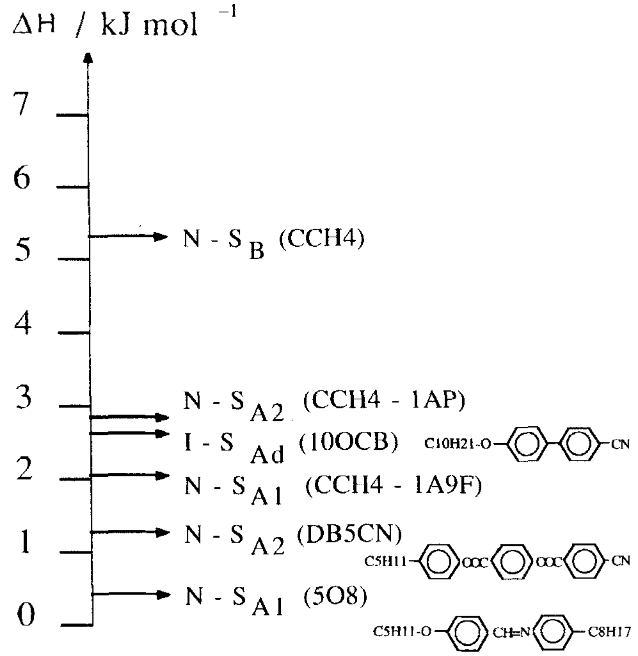

Figure 3. Comparison of the enthalpies for the S_A–N, S_A–I and S_B–N transitions in various systems.

the 100 one. The layer spacings measured in the S_{A_1} phase are surprisingly small since they are clearly less than the molecular length determined from stereomodels (see table 4); the same remark holds for the S_{A_2} phases for which the layer spacings are far from two molecular lengths. This important result implies a very peculiar structure for the lamellae which will be discussed later.

3.4. *Conclusion*

The results obtained with different techniques confirm the uncommon behaviour of these mixtures. The essential result given by the X-ray studies concerns the impossibility of comparing the thickness of the layers to a much larger molecular length. There are two ways to explain this behaviour:

(i) either an overlapping of the aliphatic parts of the molecules of two adjacent layers; but a complete interdigitation tested on stereomodels does not appear sufficient to account for the very small spacings since the chains are short;
(ii) or a tilt of the main axis of the molecules with regard to the normal to the layers without a long distance correlation of the tilt direction within the layers in order to preserve the uniaxial character of the phase [13] (which is well established by optical means as described in a forthcoming paper).

The second result of the structural analysis is the bimolecular character of the layers in most cases (S_{A_2}). However we know that the local structure of the S_{A_1} phase is very close to S_{A_2}. It is thus likely that in all of the induced S_A phases the cyano molecules are stacked head to head within the layers.

The D.S.C. measurements indicate very high enthalpies, half-way between the usual values for S_A–N transitions and the values for changes from a nematic to smectics ordered within the layers such as S_B–N transitions.

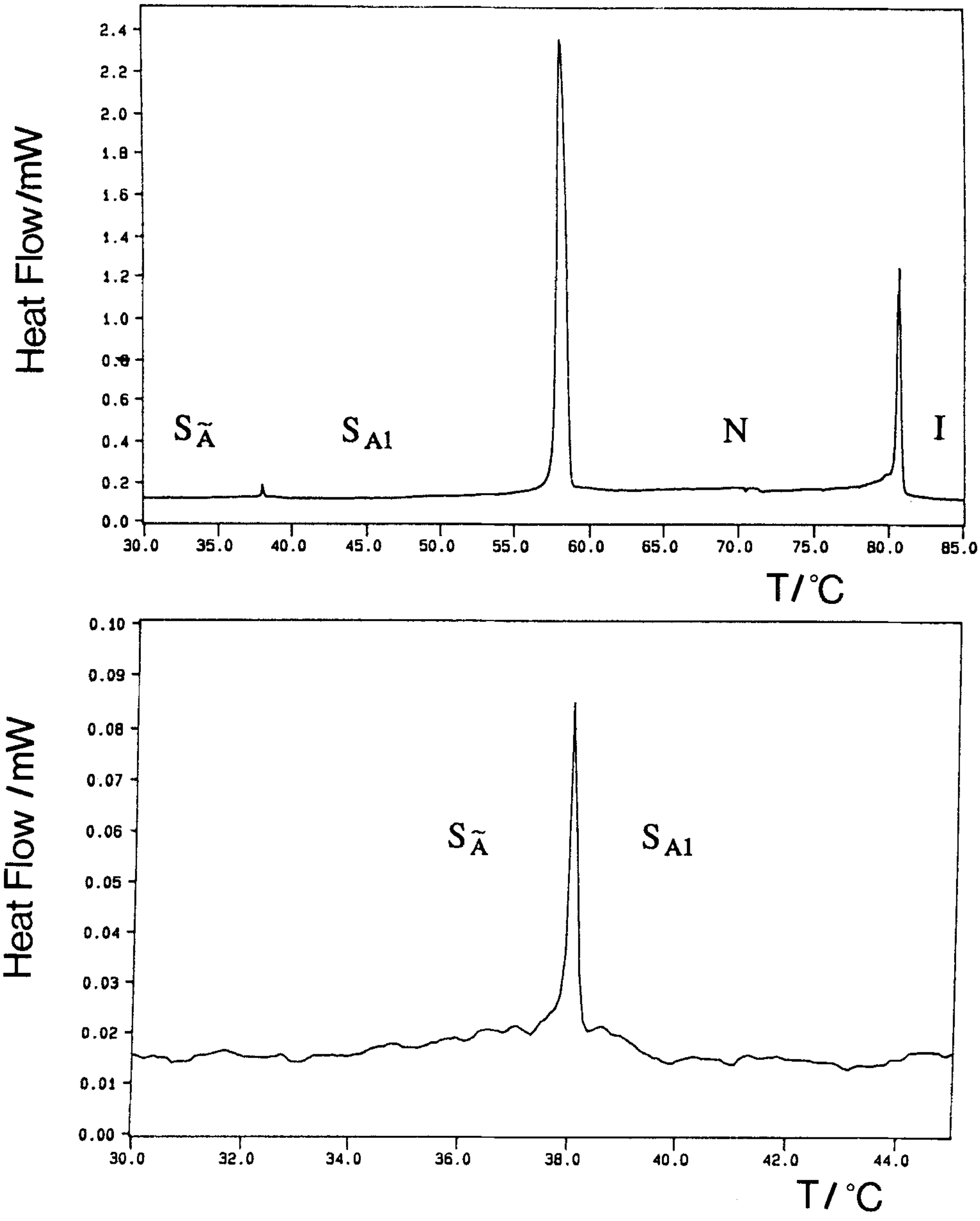

Figure 4. Thermogram for the mixture CCH4-1A9F, x_{1A9F} = 0·142, weight: 4·86 mg, heating 2°C min^{-1}.

Finally even the simple microscopic observation of a spontaneous switching from a homeotropic texture in the nematic phase to a planar texture with focal-conics in the induced smectic is unusual.

4. [*X*–*T*] phase diagrams

4.1. *Description of the diagrams*

We have chosen two systems in order to perform a complete investigation of the mixtures as a function of temperature and mole fraction. These two diagrams have

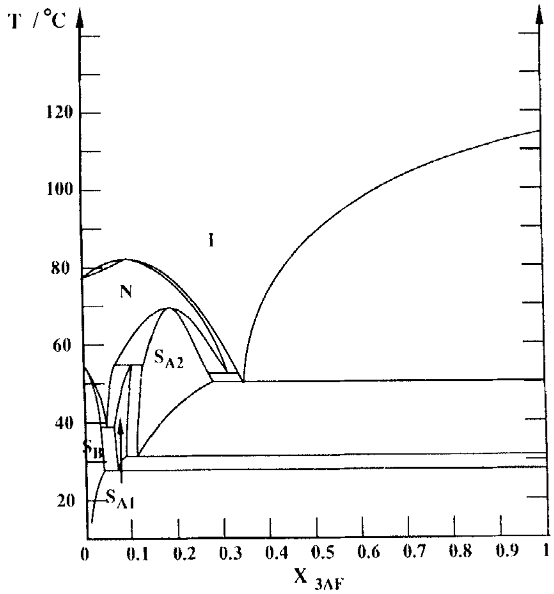

Figure 5. Isobaric phase diagram for the binary system CCH4-3AF.

been selected so that each presents an induced phase of different type, S_{A_1} and S_{A_2}. Moreover we have considered the thermal and time stability of the phases (all are enantiotropic or slightly monotropic, no important drift of the transition temperatures occurs over several days) and the better miscibility for the aromatic compound in the liquid crystal—so that it allows the study of mixtures up to the maximum of the induced phase. Two systems fulfil these conditions: CCH4-3AF (induced phase S_{A_2}); CCH4-1A9F (induced phase S_{A_1}). The phase behaviour of successive mixtures with mole fractions of the polycyclic component ranging from 0 to 0·3 has been characterized. The corresponding diagrams are represented in figures 5 and 6. Figure 7 reproduces the diagram for CCH4-1AP published in a previous paper [9].

4.2. *Discussion*

A straightforward remark is the similar forms of the three phase diagrams. The main interesting point of comparison among the diagrams regards the location of the maximum of the induced S_A–N curve with respect to the mole fraction. Whatever the system, it occurs at x of about 0·2. Then, if we move along an isotherm (for example $T = 50°C$ in CCH4-3AF, see figure 5), adding the aromatic compound destroys first the lamellar S_B crystal to give a nematic phase; further addition restores a novel lamellar order, now S_{A_1} or S_{A_2} (and an intermediate $S_{\tilde{A}}$ state with 1AP, see figure 7); an even greater concentration of the aromatic eliminates the liquid-crystalline properties and the two components are no longer miscible. In addition, the observation of different mixtures allows us to outline the large biphasic domains already noticed by the contact method.

Additional, very useful information is given by the X-ray analysis of the variation of the layer spacing as a function of the mole fraction: at constant temperature, the layer thickness does not change significantly from the S_B phase of the pure CCH4 to the induced S_A phases as evidenced by the values reported in table 5.

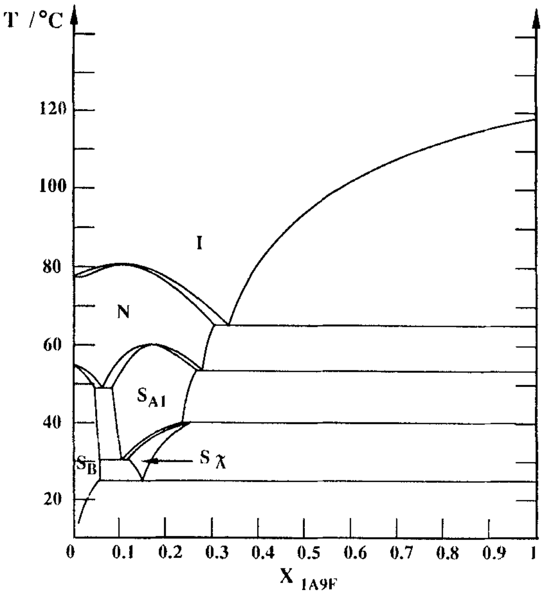

Figure 6. Isobaric phase diagram for the binary system CCH4-1A9F.

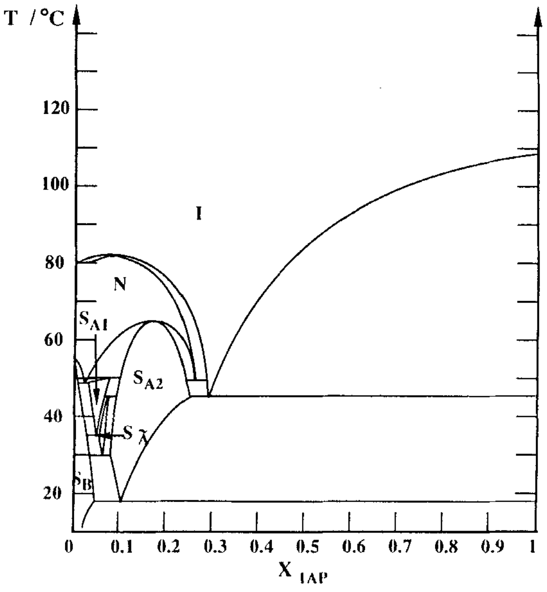

Figure 7. Isobaric phase diagram for the binary system CCH4-1AP.

5. Conclusion

This systematic study has provided a set of results which leads us to conclude that the phases induced in these systems have a very peculiar structure. However this behaviour appears limited to a narrow class of components as shown in the first part; the functionality and the molecular geometry are of equal importance for both compounds: the mesogen must bear a cyano head group and the aromatic compound an amino function. Considering these constraints in chemical nature and shape we can

Table 5. Layer thickness in the induced smectic A phase as a function of the mole fraction of the aromatic compound.

Binary system	Concentration/ mol %	d/Å
	0	28
CCH4-3AF	16·7	13·8 27·7
(S_{A_2} T = 61°C)	19·3	13·8 27·7
	0	28
CCH4-1A9F	12·4	13·9
(S_{A_1} T = 55°C)	16·7	14

imagine that donor (amine)–acceptor (cyano) interactions take place in these mixtures. A reliable explanation of the stabilization of S_A phases in most binary mixtures is the formation of complexes [6]. However, in these cases of induced phases which can be attributable to complex formation, the maximum is observed for a 0·5 mole fraction consistent with a 1–1 stoichiometry. In our diagrams this ratio is completely different since the maximum is located at 0·2, i.e. one amino aromatic molecule for four cyano mesogens.

The induced S_A phases are bimolecular (or monomolecular with a strong tendency to a local bimolecular arrangement as indicated by the occurrence of $S_{\tilde{A}}$ phases at lower temperatures). But the layer thicknesses are unexpectedly small compared to the size of the mesogens: this implies an overlapping of the layers and/or a tilt of the molecules. The spacing does not depend on the mole fraction of the aromatic component: this result allows us to rule out the possibility of a segregation of the aromatic molecules at the interfaces which would have been responsible for an expansion of the layers with concentration. Thus, although the amino compound has a totally aromatic nature, it is included inside the layers surrounded by almost fully aliphatic neighbours.

The S_A–N enthalpies of transition are unusually high. This excess heat is indicative of a more ordered structure than in conventional smectic A phases. We can assume that this order takes place within the layers but at short range since no condensation of the diffuse scattering is observed at wide angles on the X-ray patterns.

So far it is difficult to propose a model for the molecular arrangement which accounts for these observations. We have therefore performed magnetic and U.V.-visible spectroscopy experiments in order to obtain microscopic data on the respective location and orientation of the two kinds of molecules inside the layers. These results will be published in two forthcoming papers.

References

[1] Sackmann, H., and Demus, D., 1965, *Z. phys. Chem.*, **230**, 285.
[2] Sackmann, H., and Demus, D., 1963, *Z. phys. Chem.*, **224**, 177.
[3] Oh, C. S., 1977, *Molec. Crystals liq. Crystals*, **42**, 1.
[4] Domon, M., and Billard, J., 1979, *J. Phys.*, *Paris*, Coll., **40**, p. C3-413, and the references therein.

[5] DEMUS, D., HAUSER, A., PELZL, G., BÖTTGER, U., and SCHÖNBURG, S., 1985, *Crystal Res. Technol.*, **20-3**, 381.

[6] DE JEU, W. H., LONGA, L., and DEMUS, D., 1986, *J. chem. Phys.*, **84**, 6410.

[7] SIGAUD, G., ACHARD, M. F., HARDOUIN, F., and GASPAROUX, H., 1988, *Molec. Crystals liq. Crystals*, **155**, 457.

[8] ACHARD, M. F., SIGAUD, G., KELLER, P., and HARDOUIN, F., *Makromolek. Chem.*, **189**, 2159.

[9] SIGAUD, G., ACHARD, M. F., HARDOUIN, F., GASPAROUX, H., 1985, *J. Phys. Lett., Paris*, **46**, L-321.

[10] THOEN, J., BERINGHS, H., AUGUSTE, J. M., and SIGAUD, G., 1987, *Liq. Crystals*, **2**, 853.

[11] HARDOUIN, F., LEVELUT, A. M., ACHARD, M. F., and SIGAUD, G., *J. Chim. phys.*, **80**, 53.

[12] SIGAUD, G., ACHARD, M. F., HARDOUIN, F., and GASPAROUX, H., 1977, *Chem. Phys. Lett.*, **48**, 122.

[13] DE JEU, W. H., and DE POORTER, J. A., 1977, *Physics Lett.* A, **61**, 114.